Investigation of Slender-Body Vortices

John E. Fidler,* Richard G. Schwind,† and Jack N. Nielsen‡
Nielsen Engineering and Research, Inc., Mountain View, Calif.

The results of an investigation into the structure of slender missile body vortices are described. It was found that existing potential flow vortex models do not always correctly reproduce the real flow. Particularly at the base, the vorticity was found to be distributed rather than concentrated, as is usually assumed. Vortex strengths, positions, and induced velocities were predicted with only fair accuracy by the various techniques used to calculate them. It is concluded that considerable upgrading of existing models will be necessary before the strengths, locations, and induced velocities of body vortices can be predicted with certainty at high angles of attack.

Nomenclature

A = general area enclosing a region of wake vorticity
a = body radius
d = body diameter
F = vorticity flux
L = body length
ℓ = distance around contour enclosing area A
q = general velocity in crossflow plane $q=\sqrt{v^2+w^2}$
r = distance in crossflow plane measured from body axis
U,V,W = velocity components parallel to, laterally normal to, and vertically normal to body axis, respectively
V_δ = circumferential velocity at edge of crossflow boundary layer at separation
V_∞ = freestream velocity
X,Y,Z = distances parallel to, laterally normal to, and vertically normal to body axis, respectively
α = angle of attack
Γ = vortex stength
ζ = vorticity

Subscripts

B = related to body
0 = datum
V = related to vortex

Introduction

ONE of the most effective means of calculating the aerodynamic characteristics of missile configurations is by rational modeling of the flow phenomena. In this process the various features of the flowfield—uniform flows, shock waves, boundary layers, and wake vortices—are modeled mathematically and their effects on the missile calculated. Clearly, the correctness of the models used to simulate these phenomena is central to the success of the process. Considerable interplay between experiment and theory is usually necessary before satisfactory models are defined.

The present investigation was carried out to determine if the existing models used for body vortices and their flowfields are adequate. These models, which simulate the vortex strengths, positions, and detailed flow structure, are based on a mixture of analytical and semiempirical techniques. In order to attack the simplest problem first, the investigation was confined to the vortex wake formed behind a slender body at moderate-to-high angles of attack in an incompressible flow. The end result of the work was to be a body of information from which it could be determined if existing techniques were adequate for calculating vortex strengths and positions as well as the velocities induced by them in their own vicinity. All of these quantities must be predicted accurately if vortex effects are to be calculated adequately.

Present models are based on flowfield data obtained with physically intrusive probes, and some question of the possible flow distortions induced by these devices has always existed. In order to reduce to a minimum the influence of experimental equipment and technique, the flowfield surveys were made using a laser doppler velocimeter (LDV).

Attention was concentrated on the crossflow plane vortex flowfields since these exert the greatest influence on missile behavior. The tests and data analysis have already been reported in Refs. 1 and 2.

Tests and Equipment

The test was performed in the NASA/Ames Research Center 7- by 10-ft wind tunnel No. 1. The main components of the test apparatus are shown in Figs. 1 and 2. Located inside the tunnel were the missile body and its mounting, and a mirror which was mounted on the tunnel traversing mechanism (see coordinate systems in Fig. 1). The laser anemometer was located outside the tunnel, mounted on its own traversing mechanism.

The missile body used for the test was the 15.24 cm (6 in.) diam missile body of the Ames Aerodynamics Branch. It has a 3.5 length-to-diameter ratio ogive nose with a sharp point (nose apex total angle of 32.9 deg) and the same length afterbody. The sting which held the missile via the balance was a heavy-walled 5.7 cm (2¼ in.) diam tube.

The laser anemometer employed in this test was the two-component, backscatter type with a 4-W argon laser, borrowed from the Ames Large-Scale Aerodynamics Branch. The entire LDV could be traversed in the tunnel axial and vertical directions. Also, the focus point could be scanned, between 1 and 2.8 m (3.3 and 9.2 ft) from the tunnel window.

Knowledge of the flow pattern in the plane perpendicular to the missile axis was required. This meant that the LDV beams had to be turned 90 deg by a mirror in the tunnel behind the missile. The mirror needed two angular degrees of freedom for adjusting to different missile pitch angles and two translational degrees of freedom for traversing the LDV focus point. Thus, a 10×12.6 cm (4×5 in.) front-surfaced mirror was clamped to a plate and bracket to allow angular adjustments, and this was, in turn, mounted to the 7×10-ft wind-tunnel traversing mechanism (see Figs. 1 and 2). To make best use of the available range of focal length of the

Presented as Paper 77-7 at the AIAA 15th Aerospace Sciences Meeting, Los Angeles, Calif., Jan. 24-26; submitted Feb. 14, 1977; revision received Aug. 1, 1977.

Index categories: Jets, Wakes, and Viscid-Inviscid Flow Interactions; LV/M Aerodynamics; Aerodynamics.

*Engineering Management. Associate Fellow AIAA.
†Research Engineer. Member AIAA.
‡President. Fellow AIAA.

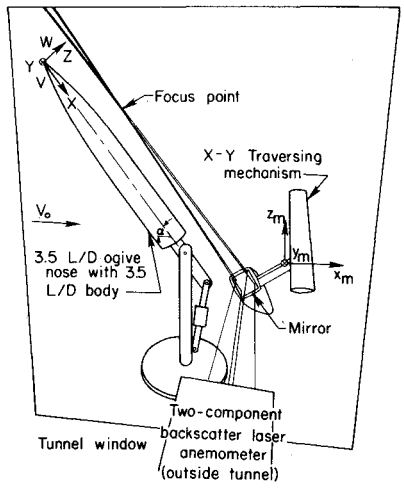

Fig. 1 Turning laser anemometer beams to obtain missile crossflow velocities.

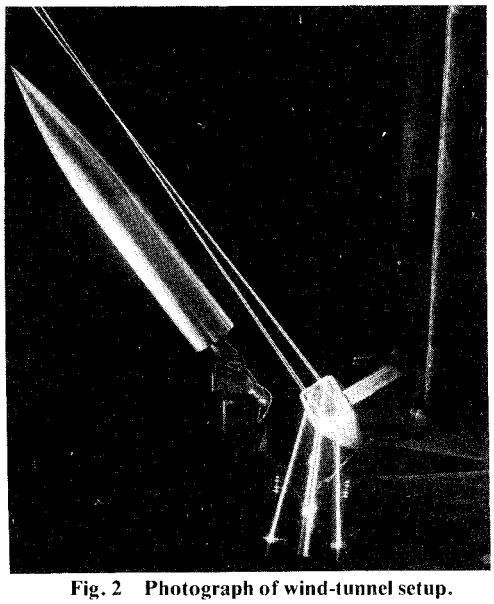

Fig. 2 Photograph of wind-tunnel setup.

LDV, the missile was placed off the wind-tunnel centerline to 0.885 m (2.90 ft), or 5.8 body diameters, from the side wall of the tunnel closest to the LDV.

A smoke generator was used to create a fog in the tunnel. This provided the particles for scattering the light of the laser beams, creating a large flux of doppler-shifted signals. It was found during testing, however, that near the vortex centers few particles were available to give appropriate signals. The particles had apparently been centrifuged out by the rotary flow. This problem is well known in LDV work.

The output of the two laser anemometer photomultiplier tubes were processed by two Hewlett Packard 141T-8443A spectrum analyzers. The peak frequency was manually selected and digitized. The three LDV and two mirror position potentiometers and the six balance gages were processed by a digital calculator to determine the LDV focus point in missile coordinates, and also the velocity and force components.

All data were obtained at a nominal freestream velocity of 18.6 m/sec (61.0 fps), which corresponds to a Reynolds number based on the missile diameter of 187,000. This velocity was selected as a compromise between decreasing LDV signal quality with increasing Reynolds number.

The LDV data were obtained at a pitch angle of 22.4 deg at the 70% and 100% axial stations. The 22.4-deg pitch angle was selected to represent one near the maximum pitch angle for formation of a symmetric vortex pair. Limited investigations at an angle of 37.5 deg were also carried out, but these are not reported here.

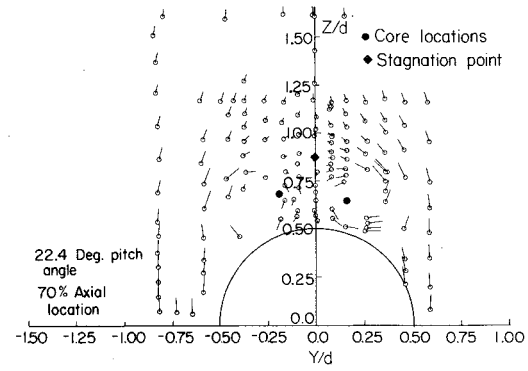

Fig. 3 Crossflow velocity field at $X/L = 0.7$.

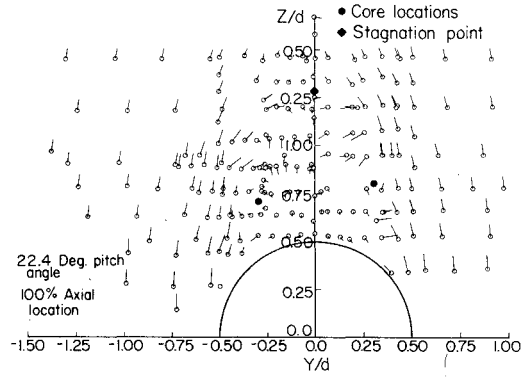

Fig. 4 Crossflow velocity field at $X/L = 1.0$.

Analysis

Velocity Fields

The symmetric vortex flowfields are shown in Figs. 3 and 4. It may be seen that at 22.4-deg angle of attack, both the 70% and 100% stations show a strong pair of vortices. The blank areas near the vortex cores at the 70% station are due to low signal-to-noise ratio associated with lack of scattering particles, which have been centrifuged out of the rapidly rotating core region.

It is interesting to note the slight asymmetries apparent in the vortex positions. The classical notion of this pattern usually envisages a perfectly symmetrical pair. However, the positions are clearly not quite symmetrical, and it will be seen later that the strengths are also slightly different. From a practical point of view, there is no reason why the vortices should be perfectly symmetrical. The asymmetries in the model and the main flowfield may be the cause.

The next steps in the analysis were the determination of the vortex strengths, positions, and associated flow velocities and the comparison of these with the predictions of existing methods. This work is described in the next section.

Symmetric Vortices

Approximately symmetric vortices were found at the 70% and 100% stations. Once the flow velocities were determined, they were then used to investigate various aspects of the flow pattern.

The first question considered was the lateral extent of the vorticity field. Two-dimensional flow photographs showed that the vortices could extend outward significantly. Accordingly, circulation was calculated around rectangular contours defined by lines extending vertically from the cylinder crest ($Z/d = 0.5$) to the upper limit of the data ($Z/d \sim 1.4$) and laterally to various vertical lines which were moved systematically outward and the circulation calculated numerically.

The results are shown in Fig. 5 for the station, $X/L = 1.0$. (This was the only station with a symmetric pair and enough

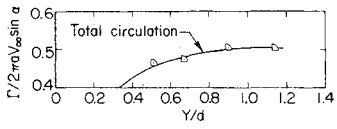

Fig. 5 Lateral variation of circulation, right-hand vortex, $X/L = 1.0$, $\alpha = 22.4$ deg.

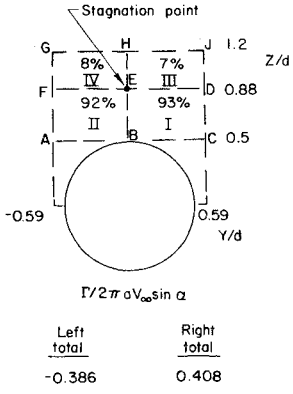

Fig. 6 Circulations from contour integrations (percentage of total in each contour), $X/L = 0.70$, $\alpha = 22.4$ deg.

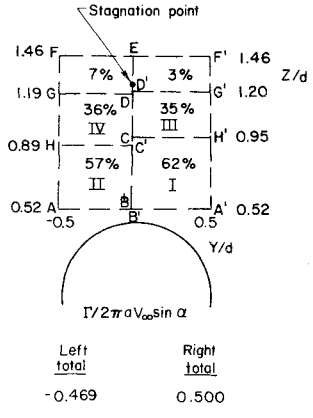

Fig. 7 Circulations from contour integrations (percentage of total in each contour), $X/L = 1.0$, $\alpha = 22.4$ deg.

information to carry out the process.) It may be seen that Γ increases as the vertical side is taken farther outward, until $Y/d \sim 1.0$ is reached. After that station, no further increase in Γ is observed. This result indicates that flowfield surveys must be taken out to at least $Y/d = 1.0$ if all of the circulation is to be captured.

If the vortices corresponded to potential vortices in which the circumferential velocity is proportional to the reciprocal of the radius from the vortex center, then they would have the property that the circulation around circuits which did not enclose the vortex center would be zero. This model is the usual basis of engineering prediction methods. In order to test this, circulation was calculated for such circuits. Because of limited data in the region of the cores, the integration contours for the 70% case could not be as extensively subdivided as for the 100% case. The results are shown in Figs. 6 and 7. It may be seen that the circulation does not correspond to the potential model. A considerable percentage of the total circulation is found away from the vortex centers. It is concluded that the vorticity is distributed rather than concentrated and that the single-point vortex model so widely used in configuration analyses is not always correct. The same result is indicated to a lesser degree by the lateral-extent investigations described earlier.

Having determined that the vorticity is distributed rather than concentrated, the next step was to compare the experimental strengths and locations with those predicted by various semiempirical and classical techniques. Locations were calculated using the following methods: 1) Föppl theory,[3] which leads to the well-known Föppl line, and 2) a semiempirical prediction based on data correlations.[4]

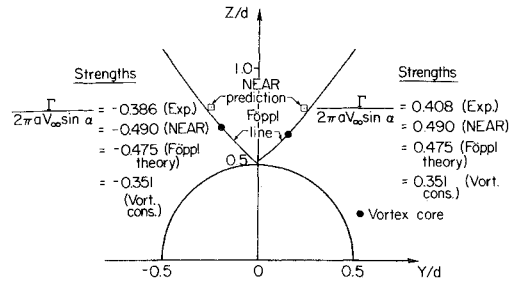

Fig. 8 Comparison of experimental and predicted vortex locations and strengths, $X/L = 0.7$, $\alpha = 22.4$ deg.

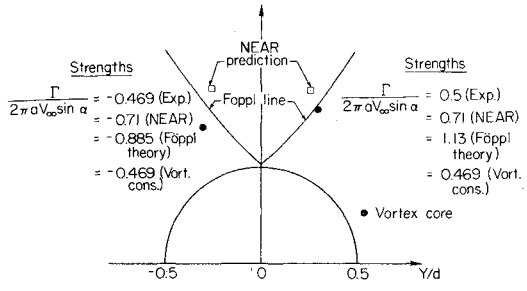

Fig. 9 Comparison of experimental and predicted vortex locations and strengths, $X/L = 1.0$, $\alpha = 22.4$ deg.

Strengths were determined from the following: 1) Föppl theory,[3] 2) a semiempirical prediction based on data correlations,[4] and 3) a semianalytical prediction based on a vorticity conservation technique.[5] A brief description will be given of each technique before comparing its prediction to the data.

Föppl Theory

It may be shown[3] that when two symmetric vortices are positioned on the lee side of a two-dimensional cylinder their centers will lie at various stationary points whose locus is a curve known as the Föppl line, the equation of which is

$$2rY = r^2 - a^2 \quad (r^2 = Y^2 + Z^2)$$

Further, to each point on the line there corresponds a vortex strength

$$\frac{\Gamma}{2\pi a(\text{vel})} = \frac{4Y^2}{a^2}\left(\frac{a}{r} + \frac{a^3}{r^3}\right)$$

where (vel) is the velocity normal to the cylinder axis, which in two dimensions is equal to the freestream velocity and in three dimensions is the crossflow velocity, $V_\infty \sin\alpha$. Thus, if the position of a vortex on the Föppl line can be determined, an estimate of its strength can be made (and vice versa).

Figures 8 and 9 show comparisons between the experimental vortex locations and the Föppl line for the cases $X/L = 0.7$ and 1.0, respectively. It will be seen that in the former case the cores lie on the line, while in the latter they lie somewhat below it. The discrepancy in the $X/L = 1.0$ case may be associated with the greater diffusion of vorticity in the vortices.

The reasonably good agreement between the Föppl line and the data is probably fortuitous to some extent. It has been observed that when vortices first appear on a slender body they are located near the crossflow boundary-layer separation line, not at the lee-side meridian as predicted by Föppl. Further, when the wake becomes asymmetric, the vortices tend to move away from the body along straight vertical lines in the crossflow plane, not along the curved Föppl line. Hence, the theory/data matching should really only occur in

the intermediate stages of vortex development, which is apparently the case here.

Using the core position r (or the point on the Föppl line nearest the core) as input to the strength equation given earlier, vortex strengths were calculated. The values are given on the figures. Comparing them with the experimental strengths shows that Föppl theory tends to overpredict these. This is unfortunate since if the strengths could have been accurately predicted by a separate technique, this would have automatically located the vortices on the Föppl line near their true positions.

Semiempirical Techniques

The procedures of Ref. 4 provide means for calculating vortex strengths and positions. The techniques are based upon correlations of experimental data. Estimates are shown in Figs. 8 and 9. It will be seen that core location is always predicted too high, while the lateral location estimate may over- or underpredict. Strength, too, is overpredicted. The technique of Ref. 4 is probably the most useful available engineering approach to calculating core locations. Some modification of the methods to increase their accuracy would be a worthwile extension of the technique.

The last technique used to predict strength is that of Ref. 5. The method will be described in some detail because of the physical insight it provides into vortex formation.

Each wake vortex is fed with vorticity from the shedding body boundary layer. The crossflow boundary-layer vorticity vectors are directed roughly parallel to the body axis. Following separation, each vortex sheet rolls up into a concentrated vortex in the wake. The vortex vorticity vectors are mainly directed parallel to the core. The rolling-up process occurs quickly, and the net vorticity shed in the boundary layer is assumed conserved while the feeding sheet rolls up into the wake vortex.

The net vorticity flux leaving the boundary layer per unit time from station X_0 to station X on the separation line is[5]

$$F_B = \Lambda \int_{X_0}^{X} \frac{V_\delta^2}{2}\,\mathrm{d}x$$

where V_δ is the circumferential velocity at the boundary-layer edge at separation, Λ is a factor (<1) accounting for the mutual annihilation of wind-side and lee-side vorticity after separation, and X_0 is the farthest upstream point to which boundary-layer separation extends. Experimental evidence indicates[5] that Λ has an approximate value of ½.

Following roll-up into a vortex whose cross section has area A bounded by contour C, the vorticity ζ proceeds downstream with the average velocity $V_\infty\cos(\alpha\text{-}2\text{ deg})$. The 2-deg figure is the approximate angle between the vortex cores and the body axis in the present tests. Hence, the flux per unit time of vorticity in a wake vortex is

$$F_V = V_\infty\cos(\alpha-2)\int_A \bar{\xi}\cdot\mathrm{d}\bar{A} = V_\infty\cos(\alpha-2)\oint_C \bar{q}\cdot\mathrm{d}\ell$$

$$= V_\infty\Gamma\cos(\alpha-2)$$

by Stokes' theorem.

Assuming that vorticity is conserved and using the value ½ for Λ yields[5]

$$\Gamma = \left[\int_{X_0}^{X} V_\delta^2\,\mathrm{d}x\right] \Big/ [4V_\infty\cos(\alpha-2)]$$

Using experimental evidence from Ref. 5 for the value of V_δ and estimating X_0 to lie at the body nose from Ref. 4, this equation may be solved for Γ. Estimates of strength are shown on Figs. 8 and 9. It will be seen that the experimental value is generally underpredicted, although the technique is the most accurate of those used.

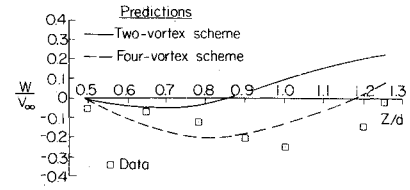

Fig. 10 Comparison of experimental and predicted vertical velocity, $Y/D=0$, $X/L=1.0$, $\alpha=22.4$ deg.

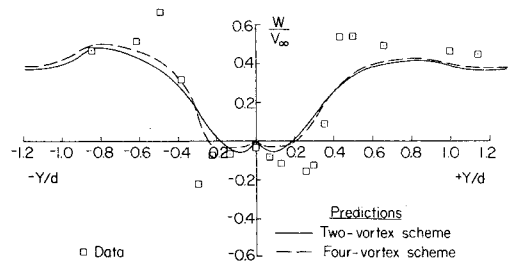

Fig. 11 Comparison of experimental and predicted vertical velocity, $Z/d=0.5$, $X/L=1.0$, $\alpha=22.4$ deg.

The next step was to determine how well the flow velocities could be predicted. Classical two-dimensional theory was used and was applied in the following two ways.

1) All of the circulation in a single vortex is lumped together at the core, regardless of the diffuse nature of the vorticity. This is termed the two-vortex model.

2) Only that fraction of the total circulation immediately associated with the core is placed there. The remainder is assumed concentrated into another vortex located above the core at the center of the area around which contour integration has been performed. In Fig. 7 one such area is *HCDG*. This arrangement is termed the four-vortex model. It should be noted that the contours were arbitrarily chosen and that almost any number could have been taken to define the same number of vortices for a multivortex model. For present purposes, however, four vortices were used. The 70% and 100% body stations will be discussed separately.

At the base (100%) the classical models were used to predict velocities along horizontal lines at $Z/d=0.5$ and 1.0 and the vertical line $Y/d=0$. The results are shown in Figs. 10-12. Along the vertical axis, Fig. 10 shows that the experimental data are not well predicted by the two-vortex model. Not only the velocities, but also the stagnation point at $Z/d=1.26$ are poorly predicted. The four-vortex model performs somewhat better, although the results are only fair. It may be that by proceeding to greater numbers of vortices even better matching could be obtained. However, such an investigation is outside the scope of the present work.

Along the line $Z/d=0.5$, Fig. 11 shows that neither the two- nor four-vortex models predict the data very well, although the gross features of the flow are correctly calculated. The major feature of the results shown here is the relative insensitivity of the prediction to the numbers of vortices. This is probably due to their relative strengths and distances from the linen insuring that the lower, stronger vortices dominate. Further, the large experimental change in W at about $Y/d=0.35$ is probably indicative of a strong feeding sheet of vorticity emanating from the boundary-layer separation point. Comparison with the flow picture of Fig. 4 bears out this conclusion. Finally, along the line $Z/D=1.0$, Fig. 12 shows that the two-vortex model again does not predict the velocities accurately. On the other hand, the four-vortex model shows good accuracy, predicting the magnitudes and trends quite well. The relative success of this model as shown in this figure and along the vertical centerline implies that it

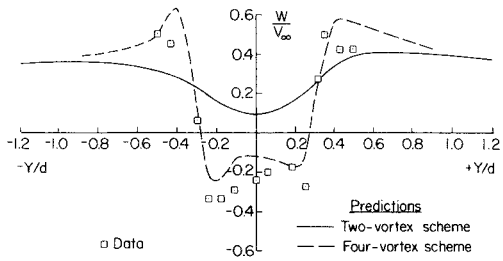

Fig. 12 Comparison of experimental and predicted vertical velocity, $Z/d = 1.0$, $X/L = 1.0$, $\alpha = 22.4$ deg.

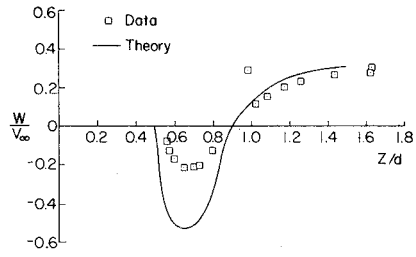

Fig. 13 Comparison of experimental and predicted vertical velocity, $Y/d = 0$, $X/L = 0.7$, $\alpha = 22.4$ deg.

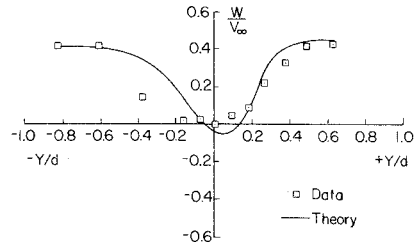

Fig. 14 Comparison of experimental and predicted vertical velocity, $Z/d = 0.88$, $X/L = 0.7$, $\alpha = 22.4$ deg.

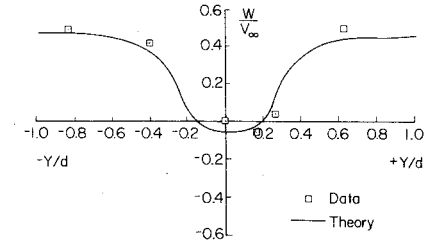

Fig. 15 Comparison of experimental and predicted vertical velocity, $Z/d = 0.5$, $X/L = 0.7$, $\alpha = 22.4$ deg.

might well be worthwhile conducting further investigations with circulation distributions to determine an optimum multivortex model for use, at least near the bases of slender bodies. The results also show that for missile applications, where the tails are typically located on a horizontal plane through the body axis, a two-vortex model might be adequate for calculating the upwash due to vortices. On the other hand, for aircraft work where T-tails are used, a four-or-more-vortex model would probably be required for upwash estimates. At the present time, however, it is not possible to determine the relative strengths and locations of the vortices in such models with certainty.

At the 70% stations only the classical two-vortex model was used to predict velocities along the horizontal lines $Z/d = 0.5$ and 0.88 and the vertical line $Y/d = 0$. The strengths and positions of the vortices in the two-vortex model were those found experimentally and shown in Fig. 9. Attention is confined to this model because of the difficulty of subdividing the contours extensively and because of its relative success in predicting the flow velocities. The first example of model performance is shown for the vertical Z axis in Fig. 13. Here it may be seen that the stagnation point is well predicted as are the flow velocities above that point. It is unlikely that any further vertical distribution of vorticity could improve significantly on this prediction. Below the stagnation point, the velocity is less well predicted, indicating that perhaps a lateral spread of the circulation could be advantageous in improving performance here. The present work does not consider such a step, but it might well be incorporated in future investigations. Turning now to the velocities along the line $Z/d = 0.88$ (which passes through the stagnation point), Fig. 14 shows that, with the exception of one or two points, these are quite well predicted by the two-vortex model. Finally, at $Z/d = 0.5$, Fig. 15 shows that the data, although sparse, are quite well predicted. Recalling the performance of the four-vortex model at the 100% station for this same horizontal line (Fig. 11), it is unlikely that such a model would improve the prediction here either.

The relative performances of the two-vortex model at the 70% and 100% stations and of the four-vortex model at 100% stations are interesting. The success of the two-vortex model at the 70% station indicates that the vortices here are more concentrated than are those at the 100% station, where a four-vortex model showed the better performance. This indicates that between the two stations some mechanism comes into play which causes the vorticity to become more distributed as it approaches the base. It is not clear what the basic cause is. However, it may well be that upstream feeding of signals from the base region plays a role in the phenomenon. It would be instructive to retest this body under the same conditions and to add further cylindrical segments aft of the base to see what this does to the flowfield. It may be possible in this way to track the development of vortex diffusion along the body. In any case, much remains to be done before a completely satisfactory model of slender-body symmetric vortices can be defined.

Conclusions

The general conclusion drawn from this investigation is that, while current concepts and models of slender-body vortices approximate the real case, considerable improvement is needed before the details of such flows and their effects on missile configurations can be adequately determined at high angles of attack. In particular:

1) The mechanism leading to distributed rather than concentrated vorticity must be studied further before satisfactory engineering models can be constructed. Whether base influence is the major contributing factor can probably be determined by testing the bodies with and without cylindrical extensions aft of the base region.

2) The vorticity distributions within diffuse vortices must be determined analytically and experimentally. This distribution should then be used to develop a multivortex model having an adequate number of vortices, appropriately distributed, to calculate the flowfield.

3) Techniques for calculating vortex strength and position must be improved. Strength calculations might be made on the basis of vorticity conservation techniques. Position estimates might be made using further correlations of experimental data.

4) Since the total vorticity in the vortices at any axial station is dependent upon the upstream feeding rate from the separation line, further investigations should deal not only with the vortical flow patterns but also with the characteristics of the body boundary layer. In particular, the separation line position should be determined as a function of axial location.

Acknowledgment

This work was supported by U.S. Army Missile Command (DRSMI-RDK) under Contract DAAH01-C-008. The authors

wish to thank K. Orloff of NASA/AMES Research Center for the use of his laser anemometer. Thanks are also due to the Large-Scale Aerodynamics Branch for use of the 7 × 10 ft wind tunnel and to the Aerodynamics Branch for use of the missile model.

References

[1]Schwind, R. G. and Kline, D. M., "Data Report on Laser Anemometer Measurements of Missile Body Separation Vortices," Nielsen Engineering and Research, TR 91, June 1975.

[2]Fidler, J. E., Schwind, R. G., and Nielsen, J. N., "An Investigation of Slender Body Wake Vortices," Nielsen Engineering and Research, TR 108, Feb. 1976.

[3]Milne-Thomson, L. M., *Theoretical Hydrodynamics*, 3rd ed., MacMillan Co., New York, 1955.

[4]Mendenhall, M. R. and Nielsen, J. N., "Effect of Vortex Shedding on the Longitudinal Aerodynamic Characteristics of Wing-Body-Tail Combinations," NASA CR-2473, Jan. 1975.

[5]Fidler, J. E., "Approximate Method for Estimating Wake Vortex Strength," *AIAA Journal*, Vol. 12, May 1974, pp. 633-635.